

Investigation of Photocatalytic Activity of Chitosan/Poly(vinyl alcohol)/TiO₂/Boron Nanocomposites

Esra BİLGİN SİMSEK *1

¹Yalova University, Engineering Faculty, Chemical and Process Engineering Department, 77100, Yalova

(Alınış / Received: 23.11.2016, Kabul / Accepted: 27.03.2017, Online Yayınlanma / Published Online: 28.04.2017)

Keywords

Photocatalytic degradation,
Catalyst,
Nanocomposite,
Pharmaceutical,
TiO₂,
Visible light

Abstract: In the current work, A series of chitosan/poly(vinyl alcohol)/TiO₂/boron nanocomposites (CS/P/Ti-B) were prepared and their activity in the photocatalytic removal of non-steroidal anti-inflammatory drug (ibuprofen (IBP)) were evaluated for the first time. The nanocomposites were characterized by scanning electron microscopy (SEM), X-ray photoelectron spectroscopy (XPS), Fourier transform infrared spectrum (FT-IR), and thermogravimetric analysis (TG-DTG). TGA thermograms showed the enhanced thermal stability of nanocomposites with increasing Ti-B content. In the photocatalytic experiments, the effects of Ti-B content, catalyst dosage and initial concentration were discussed and a suitable photodegradation process for enhanced removal was proposed. The photocatalytic removal of IBP increased with increasing Ti-B ratio and the kinetic rate constant of Ti-B increased from $4.516 \times 10^{-2} \text{ min}^{-1}$ (for raw Ti-B) to $5.346 \times 10^{-2} \text{ min}^{-1}$ (for CS/P/Ti-B/1). This increment could be attributed to the decreased recombination rate of the photo-generated electron-hole pairs.

Kitosan/Poli(vinil alkol)/ TiO₂/Bor Nanokompozitlerinin Fotokatalitik Aktivitesinin İncelenmesi

Anahtar Kelimeler

Fotokatalitik bozunma,
Katalizör,
Nanokompozit,
İlaç,
TiO₂,
Görünür ışık

Özet: Bu çalışmada, kitosan/poli vinil alkol/TiO₂/bor nanokompozitleri (CS/P/Ti-B) sentezlenmiş ve non-steroidal anti-inflamatuar ilaç (ibuprofen (IBP)) fotokatalitik giderim performansları ilk kez incelenmiştir. Nanokompozitler; taramalı elektron mikroskobu (SEM), X-ray fotoelektron spektroskopisi (XPS), Fourier Dönüşümlü Kızılötesi (FTIR) Spektroskopisi ve termogravimetrik analiz (TG-DTG) ile karakterize edilmiştir. TGA termogram sonuçlarına göre, Ti-B içeriği arttıkça nanokompozitlerin termal kararlılığının arttığı gözlenmiştir. Fotokatalitik çalışmalarda yapıdaki Ti-B içeriği, katalizör dozu ve başlangıç konsantrasyon etkisi incelenmiş ve uygun bir fotobozunma prosesi tartışılmıştır. Ti-B oranı arttıkça IBP fotokatalitik bozunma oranı artmış ve kinetik hız sabiti $4.516 \times 10^{-2} \text{ dak}^{-1}$ (saf Ti-B için) değerinden $5.346 \times 10^{-2} \text{ dak}^{-1}$ (CS/P/Ti-B/1 için) değerine yükselmiştir. Bu artış, ışın altında uyarılmış elektron boşluk çiftlerinin düşük rekombinasyon hızından kaynaklanmaktadır.

1. Introduction

In recent years, the presence of pharmaceutical residues in water has become a global concern. The non-steroidal anti-inflammatory drugs (NSAIDs) are pharmaceuticals which have been commonly detected in effluents from hospitals and urban wastewater treatment plants. Ibuprofen (IBP) was classified as one of eight pharmaceutical chemicals with fatal or chronic risks by the Organization for Economic Co-operation and Development [1].

Although IBP has hazard for human health, conventional treatment methods are ineffective to remove this pollutant [2]. Therefore, efficient treatment method should be used to remove this NSAID from the aquatic environment.

Heterogeneous photocatalysis has been applied extensively for the oxidation of various organic pollutants. Titanium dioxide (TiO₂) is the most suitable catalyst due to its chemical stability, low cost and high photoactivity [3]. However, the

photocatalytic activity of TiO₂ is limited by fast recombination of photogenerated electron (e⁻) and hole (h⁺) [4]. Many studies have been conducted to enhance the catalytic efficiency of TiO₂ by doping with metals or nonmetals [5]. Another way is to suppress the recombination of excited e⁻ and h⁺ by supporting TiO₂ on substrates such as zeolite, silica, activated carbon, alumina, and chitosan [6-8].

Due to its high mechanical strength and non-toxicity, chitosan is an effective substrate for TiO₂ in both environmental and economical ways. Chitosan is a linear polysaccharide including amino and hydroxyl functional groups. Immobilizing TiO₂ nanoparticles with chitosan could enhance the specific surface area and pore size [3, 6, 9–14]. Zainal et al. [3] showed that TiO₂-Chitosan/Glass catalyst was efficient for removing monoazo dye via the combined effect of photocatalysis-adsorption. Afzal et al. [6] synthesized TiO₂ supported chitosan nanocomposites by in-situ sol gel method and found that the reactive NH₂ and OH⁻ functional groups of chitosan were responsible for the methyl orange adsorption-photodecolorization process. Nawi et al. [11] stated that immobilized TiO₂/chitosan catalyst had attractive features like long-term stability and super oxidizing agents. Preethi et al. [12] demonstrated that the chitosan as bio template offered controlled growth of titanium via Lewis base reaction. As a result, the existence of chitosan is favorable for TiO₂ with the potential of increasing the photocatalytic activity via adsorption or via decreasing the recombination rate of electron-hole pairs.

Poly(vinyl alcohol) (PVA) is a water-soluble material with a large number of hydroxyl groups in it. Due to the distinctive intermolecular interactions and formation of hydrogen bonds between PVA and chitosan, chitosan/PVA composites have good mechanical property, adjustable pore size, favorable film- and particle-forming property and have been utilized as ideal adsorbents for removal of metal ions and organic dye from aqueous solutions [15]. On the other hand, titanium dioxide immobilized with PVA have been used as effective catalysts for photocatalytic applications [15–19]. Jiang et al. [15] synthesized mesoporous titania spheres using chitosan and PVA hydrogel and evaluated the phenol degradation. Lei et al. [19] prepared PVA/TiO₂ hybrid films as a promising recyclable TiO₂ hybrid catalysts with high photocatalytic activity.

In the current work, TiO₂ was initially doped with boron to enhance visible light response. Then, TiO₂-Boron nanoparticles were immobilized into chitosan/PVA matrix. The photocatalytic activities of composites were compared via pharmaceutical degradation under visible light. The effects of catalyst dosage and initial concentration were discussed and a suitable photodegradation process for enhanced removal was proposed.

2. Material and Method

2.1. Chemicals and reagents

All chemicals were obtained commercially and used without further purification.

2.2. Synthesis methods

2.2.1. Preparation of TiO₂/boron catalyst

Visible light-activated boron doped TiO₂ catalysts were synthesized according to the procedure as described in the previous study [20]. The weight content of boron was selected as 8.0 wt.%. Briefly, the desired amount of boric acid was dissolved in ethanol, the PEG-600 and concentrated nitric acid were added to the solution. Then, tetrabutyl titanate in ethanol was dripped into the boric acid solution and the gel was treated hydrothermally in an autoclave at 180 °C and calcined at 500 °C. The resultant sample was coded as Ti-B. The Ti-B catalyst was of well-developed anatase phase with 90.24 m²/g specific surface area and the mean pore diameter was around 10.64 nm [20].

2.2.2. Preparation of chitosan based TiO₂/boron nanocomposites

Chitosan (CS) was dissolved in 2 wt.% acetic acid solution at 25°C and left overnight with continuous mechanical stirring. Polyvinyl alcohol (PVA) with a concentration of 5 g/100 mL was dissolved in distilled water by heating the mixture at 70 °C on hot plates and stirring for about 1 h. The two solutions were then mixed at a 1:1 ratio and at room temperature using the magnetic stirrer. TiO₂-Boron powder was added into the above solution and continuously stirred to avoid aggregation of the particles. The blend solution was ultrasonically degassed to remove air bubbles, cast onto the petri dishes and dried in freeze-dryer. (TiO₂-Boron):(Chitosan/PVA) ratio was chosen as 0.5, 1.0 and 2.0 (wt.%). The composites are designated as CS/P/Ti-B/0.5, CS/P/Ti-B/1 and CS/P/Ti-B/2 according to the mass ratio of Ti-B to chitosan/PVA. The neat chitosan/PVA films were also prepared without adding Ti-B powder and coded as CS/P.

2.3. Characterization studies

The morphology of composite catalysts was examined by scanning electron microscope (SEM) equipped with a Bruker energy dispersive X-Ray (EDX) detector (Philips XL30 ESEM-FEG/EDAX). The surface functional groups were analyzed by Fourier transfer infrared (FTIR) spectrum (Perkin Elmer Spectrum One). The elemental composition of the catalysts was determined by X-ray photoelectron spectroscopy (XPS) measurements (Thermo Scientific K-Alpha X-ray Photoelectron Spectrometer). Thermogravimetric analysis (TG-

DTG) was conducted in air flow with a Simultaneous TGA–DTA Instrument (SEIKO).

2.4. Photocatalytic degradation experiments

Photocatalytic degradation studies were performed in a laboratory scale square shaped reactor equipped with two visible metal halide lamps (λ : 400–800 nm). The system is cooled through a fan at the bottom of the cabinet. For each degradation experiment, IBP solution with concentration of 10 mg/L was prepared in 50 mL double distilled water followed by adjusting the pH. Before the photocatalytic experiments, the solution was stirred for 1 h in dark to achieve adsorption equilibrium. Aliquots (5 mL) were collected at defined time intervals and filtered with 0.45 μ m syringe membrane filters. The IBP concentration was analyzed by High Performance Liquid Chromatography (Dionex Ultimate 3000 UHPLC) equipped with Acclaim C18 column (4,6 mm \times 150 mm, 3 μ m, 120 Å). The eluent used was acetonitrile/water (80/20, v/v) at a flow rate of 0.2 mL/min and the adsorption wavelength was selected as 214 nm. The effects of catalyst dosage (1.0, 2.0, 3.0 g/L), and initial concentration (10, 20, 30 mg/L) on the photocatalytic degradation were examined.

3. Results

3.1. Catalysts characterization

Figure 1 shows the SEM images of CS/P and CS/P/Ti-B nanocomposites. The smooth surface of CS/P was altered as rough surface with increasing TiO₂-Boron ratio. The Ti-B nanoparticles with dimension in the range of 16–25 nm are found as agglomerated and merged into the CS/P matrix.

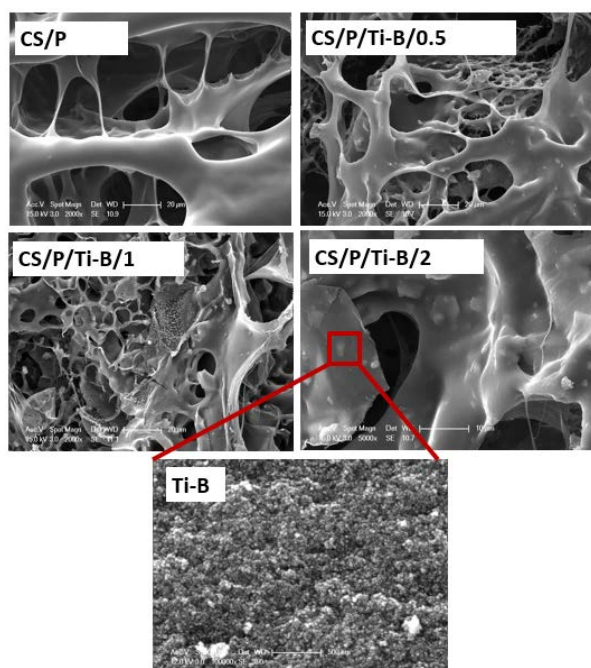


Figure 1. SEM images of samples

The EDX element mapping results of CS/P/Ti-B/2 are shown in Figure 2. The oxygen and carbon atoms formed the main structure of composite where titanium dispersed over a wide area and slight agglomeration occurred in the composite structure. Previous study [20] showed that the boron formed via Ti–O–B bonds in the TiO₂ structure. The mapping analysis (Figure 2) revealed that the boron was homogeneously dispersed in the Ti/B catalyst. The oxygen, titanium, carbon and boron contents were found as 15.7%, 22.7%, 53.8% and 7.6%, respectively.

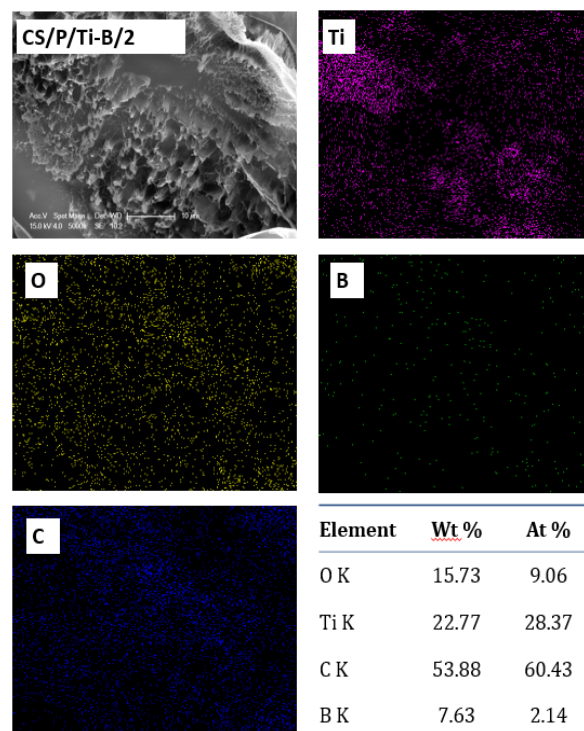


Figure 2. EDX element mappings of CS/P/Ti-B/2

In the FTIR spectra (Figure 3), the characteristic absorption bands at appeared both in raw chitosan and in nanocomposites. The broad peaks at about 3160 cm^{-1} are ascribed to the amine N–H symmetrical vibrations. The absorption peaks near 2800 cm^{-1} correspond to asymmetric stretching of C–H bonds of chitosan. The peaks at 1550 cm^{-1} ascribe to N–H deformation groups while the broad peaks at 1057 cm^{-1} are due to C–O bending vibrations. The absorption bands are also detected at 1021 cm^{-1} and 1401 cm^{-1} which are C–C and C–N stretching vibrations, respectively. Compared with raw CS/P, a new peak around 750 cm^{-1} appeared in the FTIR spectra of CS/P/Ti-B/1 and CS/P/Ti-B/2 samples corresponding to Ti–O–Ti groups. Moreover, for nanocomposite samples, the new bands at 1260 cm^{-1} were assigned to the Ti–O–C groups [19], indicating that TiO₂/Boron nanoparticles are chemically bonded to the surface of CS/P membrane rather than being adsorbed on the surface [21]. The formation of covalent Ti–O–C bonds also revealed the effective immobilization of Ti/B nanoparticles in CS/P matrix [19].

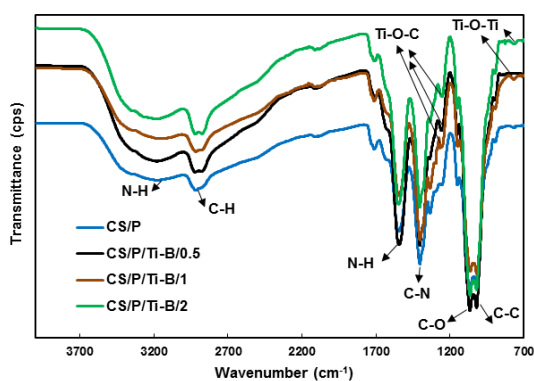


Figure 3. FTIR spectra of samples

As the thermogravimetric analysis is considered as the most essential method for studying thermal stability of polymers, the influence of the TiO₂/B crystal structure on the polymer template was examined by TGA. The results are shown in Figure 4. The weight loss of 9.5% at 50–100°C is due to the moisture vaporization. The other weight loss at 200–300°C is due to the decomposition of chitosan chain.

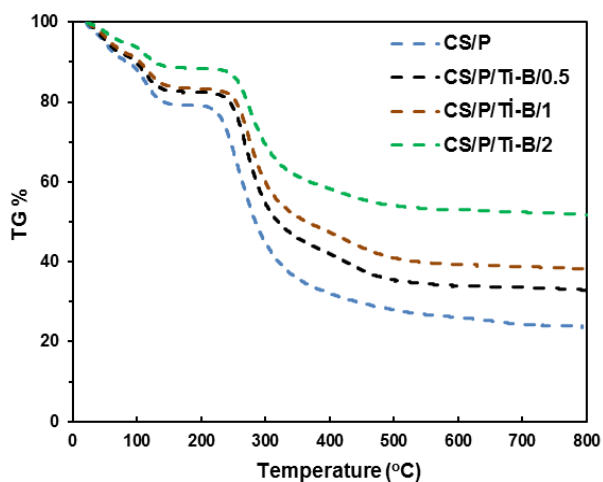


Figure 4. TGA results of samples

When temperature increased, the raw CS/P was not thermally stable and 75% of the sample decomposed before 600°C. For CS/P/Ti-B/2 nanocomposite, a weight loss of 5.2% at 50–100°C is due to the evaporation of water. The second stage starts at 200–400°C with a weight loss of 29.7% due to the thermal and oxidative decomposition of composite. The residual mass at 800 °C were found as 32.9%, 38.1% and 51.7% for CS/P/Ti-B/0.5, CS/P/Ti-B/1 and CS/P/Ti-B/2 catalysts, respectively. With the increase in Ti-B content, the weight-loss decreased gradually indicating the enhanced thermal stability of nanocomposites. This could be attributed to the crystalline regions and Ti-O-C chemical bonds which act as crosslinking sites to keep CS/PVA stable [19].

In order to examine the surface compositions of raw CS/P and CS/P/Ti-B composites, X-ray photoelectron spectroscopy (XPS) was conducted. As seen in Figure 5, all samples have main peaks at 531.9 eV, 285 eV and 399 eV corresponding O 1s, C 1s and N 1s chemical states, respectively. After doped with Ti-B

nanoparticles, Ti 2p peak was located at about 458 eV confirming the presence of Ti⁴⁺ in the chitosan/PVA matrix. However, no peaks of boron were detected owing to the small quantity of boron in the structure.

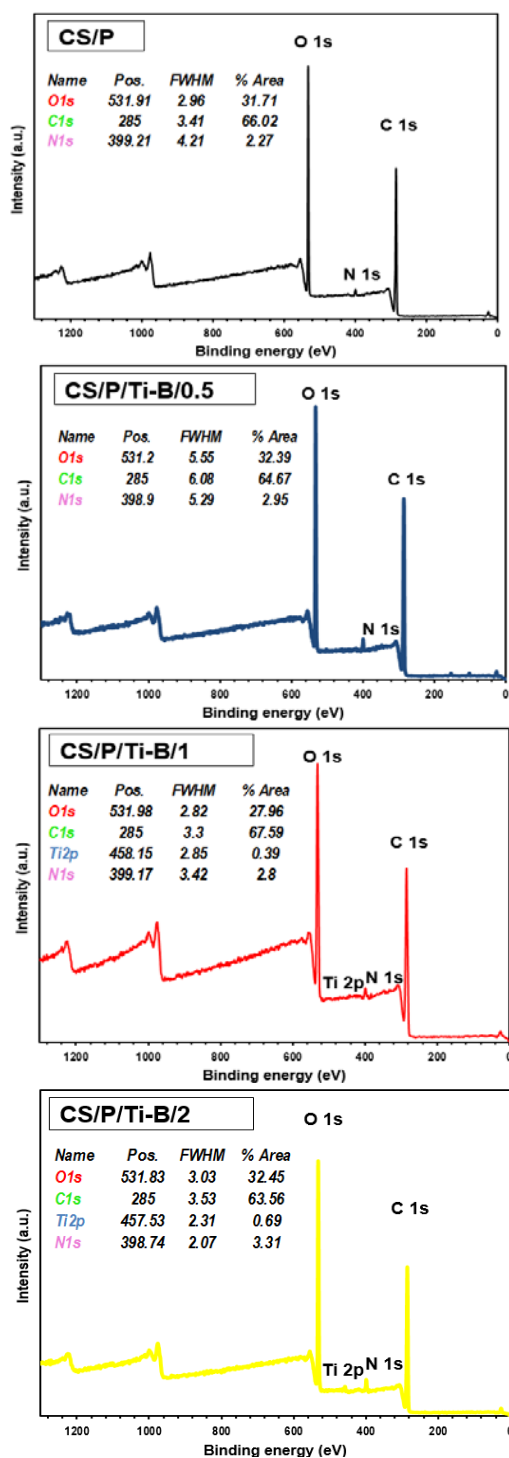


Figure 5. XPS spectra of samples

3.2. Photocatalytic studies

Photocatalytic degradation experiments were conducted with raw CS/P and CS/P/Ti-B composites under visible light illumination. The IBP solution with concentration of 10 mg/L were illuminated with 2 g/L catalyst at natural pH~6.5 and the results are represented in Figure 6.

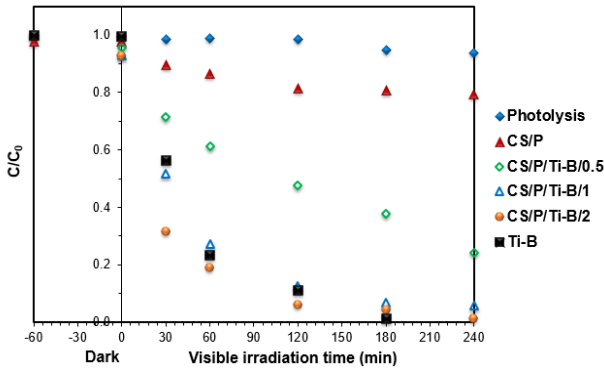


Figure 6. Photodegradation of IBP ($C_i = 10$ mg/L, Catalyst dose: 2 g/L, pH 6.5)

Under visible light irradiation no degradation of IBP was observed in the absence of catalyst over a period of 240 min. To ensure the adsorption performance, IBP was treated with raw CS/P sample and at the end of 4 h, 20.4% removal was achieved. After 3 h treatment with composites under visible light, the degradation rate of CS/P/Ti-B/0.5, CS/P/Ti-B/1 and CS/P/Ti-B/2 were 62.3%, 93.1% and 95.7%, respectively. The high photocatalytic activity of CS/P/Ti-B/2 composite due to the synergistic effect of the photocatalysis and adsorption [9, 11, 22]. Since the adsorption efficiency of CS/P can result in higher concentration of IBP molecules near the catalyst, the adsorption performance of CS/P plays an important role for the enhancement in the photodegradation over CS/P/Ti-B catalyst. In addition, the main factor affecting the enhanced degradation could be due to the decreased recombination rate of the photo-induced electron-hole pairs which was achieved with introducing TiO₂/B into the chitosan/PVA matrix.

It is observed that CS/P/Ti-B/2 nanocomposite shows higher photocatalytic efficiency when compared with Ti/B powder. At the end of 2 h, the removal efficiency of IBP by CS/P/Ti-B/2 is calculated to be 93.9%, which is about 1.05 times of Ti/B (89.1%). On the other hand, CS/P/Ti-B/1 shows similar photocatalytic performance with Ti/B powder. Due to the practical drawbacks of using powder catalyst, such as agglomeration during utility and difficulty in separating from treated effluent [15], CS/P/Ti-B composite is a good alternative to remove organic pollutants from aqueous solution.

Table 1. The rate constants k_{app} and R^2 values of samples

	$k_{app} \times 10^{-2}$ (min ⁻¹)	R^2
Ti-B	4.516	0.908
CS/P	3.296	0.863
CS/P/Ti-B/0.5	2.053	0.973
CS/P/Ti-B/1	5.346	0.949
CS/P/Ti-B/2	6.650	0.963

The Langmuir–Hinshelwood kinetic model was used in order to examine the photocatalytic removal:

$$r = k_c \theta = -\frac{d[C]}{dt} = k_c \frac{K_c [C]}{1 + K_c [C]} \quad (1)$$

where r is the rate of degradation, K_c and k_c reflect the adsorption equilibrium and kinetic constants, respectively. At low initial concentrations, the term $K_c C$ in the denominator can be neglected with respect to unity and the rate becomes, apparently, first order:

$$r = -\frac{d[C]}{dt} = k_c K_c C = k_{app} C \quad (2)$$

where k_{app} (min⁻¹) is the apparent rate constant. After integration of Eq.(2) within the limits of $t=0 \rightarrow t=t$ and $[C]=[C]_0 \rightarrow [C]=[C]$; the equation can be expressed as:

$$-\ln\left(\frac{C}{C_0}\right) = k_{app} t \quad (3)$$

where C and C_0 are the IBP concentrations at time t and at the start of the degradation, respectively. The rate constants for IBP degradation are shown in Table 1. The IBP photodegradation was enhanced significantly with increasing the (Ti-B): (CS/P) ratio from 0.5 to 2.0. The highest kinetic constant (6.650×10^{-2} min⁻¹) was obtained with CS/P/Ti-B/2 nanocomposite. Moreover, the k_{app} value of Ti-B increased from 4.516×10^{-2} min⁻¹ to 5.346×10^{-2} min⁻¹ when the CS/P/Ti-B/1 catalyst was used.

3.2.1. Effect of catalyst dosage

In the photocatalytic process, the catalyst dosage should be optimized for maximum degradation since it may effect in unfavorable light scattering and decrease the photon absorption efficiency. The effect of catalyst dosage on the degradation of IBP was studied with the dosages varied from 1.0 g/L to 3.0 g/L.

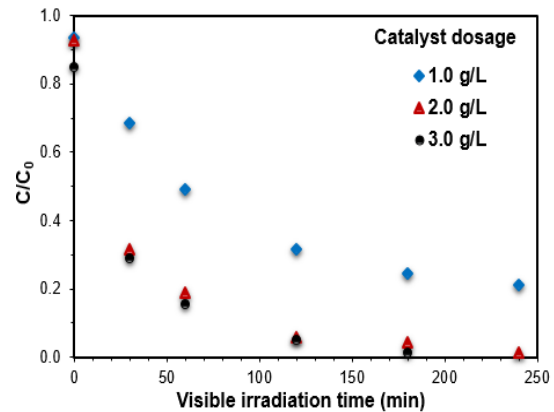


Figure 7. Effect of catalyst dosage on IBP degradation ($C_i = 10$ mg/L)

As seen in Figure 7, at the end of 3 h, when the catalyst dosage increased from 1.0 g/L to 2.0 g/L, the

degradation efficiency increased from 78.3% to 95.7%. This increase could be ascribed to the increment in the active sites available for IBP degradation. However, further increase has a slight effect on the IBP removal which could be attributed to the difficult light penetration with catalyst agglomeration [23]. Consequently, 2.0 g/L catalyst loading was chosen as optimum for further experiments.

3.2.2. Effect of initial concentration

Figure 8 shows the effect of varying initial concentration on IBP degradation by CS/P/Ti-B/2 catalyst. IBP solution with 10 mg/L concentration was degraded at a faster rate than 20 mg/L and 30 mg/L solutions. The IBP removal decreased from 98.6% to 76.8% when the initial concentration increased from 10 mg/L to 30 mg/L. The decrease can be ascribed to the saturation of the photocatalytic active sites by higher concentration of substrate and reduction the photons interaction [12, 24]. Due to the saturation, the drug molecules cannot easily contact with the photo-induced holes of catalyst [25]. On the other hand, with increasing initial concentration, more IBP molecules were adsorbed on the catalyst surface, and the generation of OH radicals at the catalyst surface was reduced since the active sites were occupied by IBP molecules [24, 26].

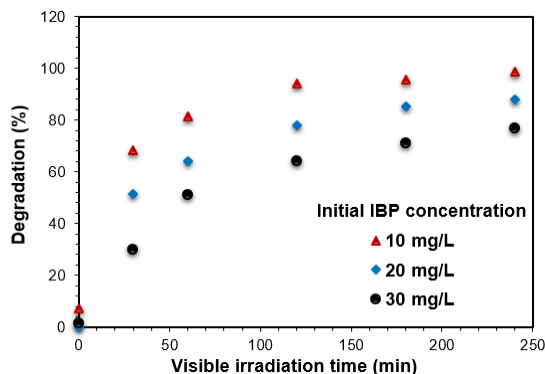


Figure 8. Effect of IBP concentration on the photocatalytic degradation (Catalyst dose: 2 g/L)

4. Discussion and Conclusion

Photocatalytic degradation of a non-steroidal anti-inflammatory drug, ibuprofen (IBP) was first investigated by using chitosan/poly(vinyl alcohol)/TiO₂/Boron nanocomposites. Boron doped TiO₂ catalysts were prepared by solvothermal method and then immobilized into chitosan/poly(vinyl alcohol) matrix. SEM images revealed that the smooth surface of CS/P was altered as rough surface with increasing TiO₂-Boron ratio. EDX and SEM mapping analysis demonstrated the presence of titanium and boron elements in the polymer matrix. TGA thermograms showed the enhanced thermal stability of nanocomposites with increasing Ti-B content. The photocatalytic

experiments were conducted under visible light irradiation. The IBP photocatalytic removal was found higher with increasing Ti-B ratio which could be attributed to the decreased recombination rate of the photo-generated electron-hole pairs.

Acknowledgment

Author is grateful to A. Akan for the kind help on the HPLC measurements. Author appreciates the reviewers for their kind comments and suggestions to improve this manuscript.

References

- [1] Kang, K., Jang, M., Cui, M., Qiu, P., Park, B. 2014. Preparation and characterization of magnetic-core titanium dioxide: Implications for photocatalytic removal of ibuprofen. *Journal of Molecular Catalysis A: Chemical*, 390, 178–186.
- [2] Tran, N., Drogui, P., Nguyen, L., Brar, S.K. 2015. Optimization of sono-electrochemical oxidation of ibuprofen in wastewater. *Journal of Environmental Chemical Engineering*, 3, 2637–2646.
- [3] Zainal, Z., Hui, L.K., Hussein, M.Z., Abdullah, A.H., Hamadneh, I.R. 2009. Characterization of TiO₂-Chitosan/Glass photocatalyst for the removal of a monoazo dye via photodegradation-adsorption process. *Journal of Hazardous Materials*, 164, 138–145.
- [4] Shi, J.W. 2009. Preparation of Fe(III) and Ho(III) co-doped TiO₂ films loaded on activated carbon fibers and their photocatalytic activities. *Chemical Engineering Journal*, 151, 241–246.
- [5] Choina, J., Fischer, C., Flechsig, G.U., Kosslick, H., Tuan, V.A., Tuyen, N.D., Tuyen, N.A., Schulz, A. 2014. Photocatalytic properties of Zr-doped titania in the degradation of the pharmaceutical ibuprofen. *Journal of Photochemistry and Photobiology A: Chemistry*, 274, 108–116.
- [6] Afzal, S., Samsudin, E.M., Muna, L.K., Julkapli, N.M., Hamid, S.B.A. 2017. Room temperature synthesis of TiO₂ supported chitosan photocatalyst: Study on physicochemical and adsorption photo-decolorization properties. *Materials Research Bulletin*, 86, 24–29.
- [7] Pucher, P., Benmami, M., Azouani R., Krammer, G., Chhor, K., Bocquet, J.-F., Kanaev, A.V. 2007. Nano-TiO₂ sols immobilized on porous silica as new efficient photocatalyst. *Applied Catalysis A: General*, 332, 297–303.
- [8] Huang, M., Xu, C., Wu, Z., Huang, Y., Lin, J., Wu, J. 2008. Photocatalytic discolorization of methyl orange solution by Pt modified TiO₂ loaded on natural zeolite, *Dyes Pigments*, 77, 327–334.
- [9] Zhang, J., Wang, X., Bu, Y., Wang, X., Song, J., Xia, P., Ma, R., Louangsouphom, B., Ma, S., Zhao, J.

2016. Remediation of diesel polluted water through buoyant sunlight responsive iron and nitrogen co-doped TiO₂ coated on chitosan carbonized fly ash. *Chemical Engineering Journal*, 306, 460–470.
- [10] Dhanya, A., Aparna, K. 2016. Synthesis and Evaluation of TiO₂/Chitosan based hydrogel for the Adsorptional Photocatalytic Degradation of Azo and Anthraquinone Dye under UV Light Irradiation. *Procedia Technology*, 24, 611 – 618.
- [11] Nawi, M.A., Jawad, A.H., Sabar, S., Wan Ngah, W.S. 2011. Immobilized bilayer TiO₂/chitosan system for the removal of phenol under irradiation by a 45 watt compact fluorescent lamp. *Desalination*, 280, 288–296.
- [12] Preethi, T., Abarna, B., Rajarajeswari, G.R. 2014. Influence of chitosan-PEG binary template on the crystallite characteristics of sol-gel synthesized mesoporous nano-titania photocatalyst. *Applied Surface Science*, 317, 90–97.
- [13] Yang, D., Li, J., Jiang, Z., Lu, L., Chen, X. 2009. Chitosan/TiO₂ nanocomposite pervaporation membranes for ethanol dehydration. *Chemical Engineering Science*, 64, 3130–3137.
- [14] Samadi, S., Khalilian, F., Tabatabaee, A. 2014. Synthesis, characterization and application of Cu-TiO₂/chitosan nanocomposite thin film for the removal of some heavy metals from aquatic media. *Journal of Nanostructure in Chemistry*, 4, 84.
- [15] Jiang, R., Zhu, H.-Y., Chen, H.-H., Yao, J., Fu, Y.-Q., Zhang, Z.-Y., Xu, Y.-M. 2014. Effect of calcination temperature on physical parameters and photocatalytic activity of mesoporous titania spheres using chitosan/poly(vinyl alcohol) hydrogel beads as a template. *Applied Surface Science*, 319, 189–196.
- [16] Hegedus, P., Szabó-Bárdos, E., Horváth, O., Szabó, P., Horváth, K. 2017. Investigation of a TiO₂ photocatalyst immobilized with poly(vinyl alcohol). *Catalysis Today*, 284, 179–186.
- [17] Habiba, U., Islam, S., Siddique, T.A., Afifi, A.M., Chin, B. 2016. Adsorption and photocatalytic degradation of anionic dyes on Chitosan/PVA/Na-Titanate/TiO₂ composites synthesized by solution casting method. *Carbohydrate Polymers*, 149, 317–331.
- [18] Abd El-Rehim, E.S.A. 2012. Photo-catalytic degradation of metanil yellow dye using TiO₂ immobilized into polyvinyl alcohol/acrylic acid microgels prepared by ionizing radiation. *Reactive and Functional Polymers*, 72, 823–831.
- [19] Lei, P., Wang, F., Gao, X., Ding, Y., Zhang, S., Zhao, J., Liu, S., Yang, M. 2012. Immobilization of TiO₂ nanoparticles in polymeric substrates by chemical bonding for multi-cycle photodegradation of organic pollutants. *Journal of Hazardous Materials*, 227–228, 185–194.
- [20] Bilgin Simsek, E. 2017. Solvothermal synthesized boron doped TiO₂ catalysts: Photocatalytic degradation of endocrine disrupting compounds and pharmaceuticals under visible light irradiation. *Applied Catalysis B: Environmental*, 200, 309–322.
- [21] Hasmath Farzana, M., Meenakshi, S. 2015. Photocatalytic aptitude of titanium dioxide impregnated chitosan beads for the reduction of Cr(VI). *International Journal of Biological Macromolecules*, 72, 1265–1271.
- [22] Nawi, M.A., Sabar, S., Jawad, A.H., W.S.W. Ngah Sheilatina. 2010. Adsorption of reactive Red 4 by immobilized chitosan on glass plate: towards the design of immobilized TiO₂-chitosan synergistic photocatalyst-adsorption bilayer system. *Biochemical Engineering Journal*, 49, 317–325.
- [23] Vaiano, V., Iervolino, G., Sannino, D., Rizzo, L., Sarno, G., Farina, A. 2014. Enhanced photocatalytic oxidation of arsenite to arsenate in water solutions by a new catalyst based on MoO_x supported on TiO₂. *Applied Catalysis B: Environmental*, 160–161, 247–253.
- [24] Bechambi, O., Sayadi, S., Najjar, W. 2015. Photocatalytic degradation of bisphenol A in the presence of C-doped ZnO: Effect of operational parameters and photodegradation mechanism. *Journal of Industrial and Engineering Chemistry*, 32, 201–210.
- [25] Gu, L., Chen, Z., Sun, C., Wei, B., Yu, X. 2010. Photocatalytic degradation of 2,4-dichlorophenol using granular activated carbon supported TiO₂. *Desalination*, 263, 107–112.
- [26] Nezamzadeh-Ejhieh, A., Karimi-Shamsabadi, M. 2013. Decolorization of a binary azo dyes mixture using CuO incorporated nanozeolite-X as a heterogeneous catalyst and solar irradiation, *Chemical Engineering Journal*, 228, 631–641.